



Sea-surface partial pressure of carbon dioxide in the eastern
equatorial Pacific (August 1991 to October 1992): A multivariate
analysis of physical and biological factors

YVES DANDONNEAU*

(Received 1 March 1994; in revised form 20 September 1994; accepted 15 July 1995)

Abstract—Underway PCO_2 measurements were made every three months from a merchant ship in the equatorial Pacific Ocean. The shipping track from Panama to Tahiti crosses the equator near 100°W , collecting PCO_2 , sea surface temperature (SST), fluorescence of chlorophyll, nitrate concentration and depth of the mixed layer. The survey started in August 1991, with strong upwelling conditions and PCO_2 peaking at $484 \mu\text{atm}$ right at the equator. Equatorial warming in November 1991 and decreased upwelling occurred with maximum PCO_2 at $460 \mu\text{atm}$, at $2^\circ 30'\text{S}$. With the advent of the 1992 El Niño, and the collapse of equatorial upwelling, PCO_2 was drastically reduced in March 1992. The maximum of PCO_2 was only $397 \mu\text{atm}$ at $0^\circ 40'\text{S}$, and values greater than $380 \mu\text{atm}$ spread southward to 6°S . Nitrate concentration, however, was still high between the equator and 10°S . With return to normal conditions in June 1992, PCO_2 rose to $437 \mu\text{atm}$ at $2^\circ 30'\text{S}$, and in October 1992 strong upwelling brought CO_2 -rich water to the surface, with maximum PCO_2 at $0^\circ 12'\text{N}$, at $480 \mu\text{atm}$.

Multivariate analysis of the data between 7°N and 20°S , after normalization, shows that 60% of the total variance could be explained by the first eigenvector, in which PCO_2 , nitrate and fluorescence were opposed to SST. The empirical orthogonal function (EOF) associated to this eigenvector was maximum at or near the equator and decreased abruptly to the north but gradually to the south. This EOF and the corresponding eigenvector could be interpreted as a synthetic representation of the influence of upwelling and of the main processes that modify PCO_2 : biological carbon uptake and heating. The variations of the depth of the mixed layer (taken as the depth where temperature was 1°C below SST) were uncorrelated with PCO_2 . A strong correlation ($r = 0.97$, $n = 5$) was found between the temperature of upwelled waters (i.e. the minimum SST observed near the equator) and the average PCO_2 between 0° and 5°S .

INTRODUCTION

The equatorial Pacific has long been recognized as an important source area for the global budget of air-sea CO_2 exchange (Keeling, 1968; Broecker *et al.*, 1986; Murphy *et al.*, 1991; Lefevre and Dandonneau, 1992). In this area, the partial pressure of carbon dioxide in surface seawater (PCO_2) is higher than that in the atmosphere (pCO_2) due to the equatorial upwelling of CO_2 -rich deep waters. The tongue of cold upwelled water (Wyrtki, 1981) that spreads westwards from the coast of America is also known to vary inversely with the strength of the El Niño–Southern Oscillation (ENSO) events. Most properties of equatorial surface seawater are deeply affected by ENSO (Philander, 1989), including PCO_2 , which decreases during the warming period (Inoue and Sugimura, 1992; Wong *et*

*LODYC (Unité mixte de recherche CNRS-ORSTOM-UPMC), Tour 14, 2^{ème} étage, Université Pierre et Marie Curie, 4, Place Jussieu, 75252 Paris cedex 05, France.

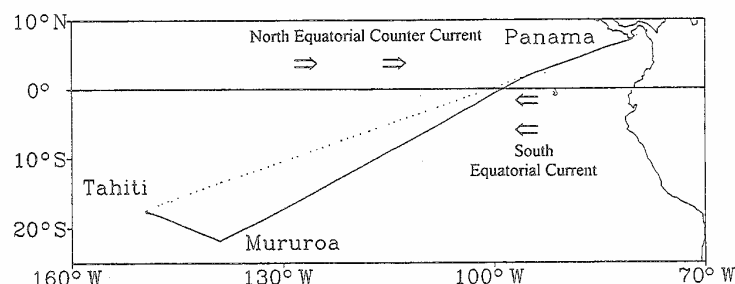


Fig. 1. The route followed by M/V. *Le Rabelais* from Panama to Tahiti. Continuous line: transects made in August and November 1991, and in March and June 1992. Dotted line: transect made in October 1992.

al., 1993; Feely *et al.*, 1995). The low winds that prevail along the equator during the warm events, associated to abnormally low PCO_2 , result in a reduced sea to air CO_2 flux (Inoue and Sugimura, 1992), causing a large decrease in the rate of CO_2 accumulation in the atmosphere during the early stage of El Niño events, followed by a sharp increase during the mature stage (Bacastow *et al.*, 1980; Wong *et al.*, 1984; Gaudry *et al.*, 1991; Keeling and Revelle, 1985).

Upwelling of cold, nutrient-rich water in the equatorial Pacific Ocean supplies high PCO_2 ($>450 \mu\text{atm}$) (Feely *et al.*, 1987). According to Wyrski (1981), upwelled waters reaching the surface between 2°S and 2°N originate from the upper part of the Equatorial Undercurrent, at ~ 50 m depth in the east, and ~ 150 m at 170°W (Eldin and Morliere, 1992). Divergent flow of the South Equatorial Current further spreads these waters poleward, and heating results in a decrease of CO_2 solubility (Weiss, 1974) so that PCO_2 would normally increase. However, at the same time, intense photosynthesis favoured by newly upwelled nitrate takes up CO_2 at such a rate that a downstream increase of PCO_2 is generally not observed (Lefevre *et al.*, 1994). Equatorial instability waves, mixing, and CO_2 exchange with the atmosphere, further complicate the variations of PCO_2 that are not yet completely understood.

We started to collect PCO_2 data on the commercial shiptrack from Le Havre (France) to Nouméa (New Caledonia) in August 1991, in order to describe and understand the variability of PCO_2 , and thus improve the predictability of air-sea CO_2 exchange in the equatorial Pacific (program ECOA: Exchange of Carbon between the Ocean and the Atmosphere). The shiptrack covers the equatorial Pacific from Panama to Tahiti or Mururoa (French Polynesia), crossing the equator at about 100°W (Fig. 1). The first five transects (cruises ECOA 1 to 5) were made in August 1991, November 1991, March 1992, June 1992 and October 1992, starting in normal conditions, in Austral winter, and through the El Niño, which started during the northern winter 1991–1992. The PCO_2 data from these transects, which complemented those collected during the US JGOFS EqPac cruises (Murray *et al.*, 1992), are presented here, together with chlorophyll *a* fluorescence, temperature and nitrate variations.

METHODS

Shipboard measurements of PCO_2 , pCO_2 , fluorescence, temperature, and sampling for chlorophyll *a* and nitrate were carried out as described below, from a container-carrier:

M/V *Le Rabelais* (formerly M/V *Lillooet*, in Wong *et al.*, 1993). A scientific observer embarked on each trip to watch over the equipment and conduct calibrations and sampling.

PCO₂ measurements

The CO₂ measuring system included an air-sea equilibration, a series of water vapour traps, computer-controlled valves, a membrane air pump and an infra-red CO₂ analyser (Fig. 2).

Seawater at the intake of sea chests below sea level was pumped up to the laboratory, at about 15 m above sea level. It then entered the equilibration vertically through a "water pump", or "water flow aspirator", commonly used to produce vacuum for filtration purposes (i.e. a "T" tube which produces sucking on the branch C at a right angle when water flows through the two vertical branches A and B in line; see Fig. 2). This equilibrator is different from those based either on a shower (Keeling *et al.*, 1965; Murphy *et al.*, 1991; Wong *et al.*, 1993), or on bubbling (Copin-Montegut, 1985), and in fact, combines both types:

- Water enters the "water pump" through branch A at 2 bar pressure, 10 l min⁻¹.
- Widening out of the outlet (branch B) produces sucking in the branch C at a right angle, to mix air in tiny bubbles into the flowing seawater. Air flow rate through the "water pump" is about 10 l min⁻¹.
- Seawater is then injected into a Plexiglas box, 25 × 25 × 5 cm, with staggered walls, in which air and seawater separate.
- The air flow through the CO₂ infrared analyser is adjusted to 0.8 l min⁻¹, which is much less than the 10 l min⁻¹ air flow through the "water pump". To maintain an even flow, air inside the Plexiglas® box is recycled through the "water pump", resulting in an efficient equilibration loop (on the average, air passes 10/0.8 ≈ 12 times through this loop before going to the CO₂ infrared analyser).
- The air circuit during cruises ECOA 1 to 5 was an open one, in which air was not

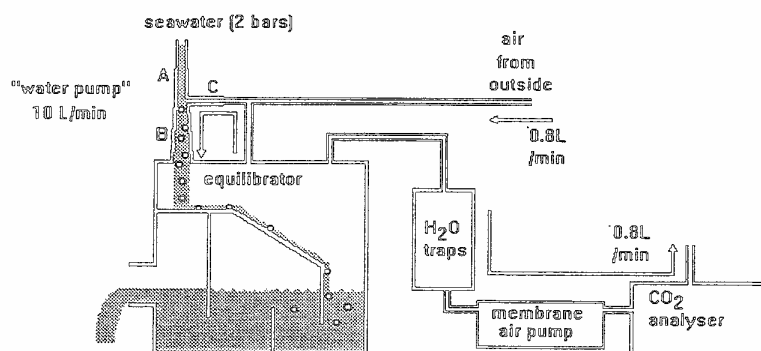


Fig. 2. Schematic representation of the air-sea CO₂ equilibration system. Equilibrium is achieved in the air loop (10 l min⁻¹) between the "water pump" and the upper compartment of the equilibrator. The circuits for atmospheric pCO₂ measurement and calibration gases, the valves, and temperature and pressure sensors are not represented for the sake of simplicity.

recirculated after passing through the CO₂ infrared analyser. The efficiency of the equilibrator was tested by equilibrating seawater with air from two different sources with known CO₂ concentration (air taken outside, and a gas standard at ~700 ppm). One hundred per cent efficiency would give the same [CO_{2 sea}] value for both gases. We found a slight difference, giving efficiency = 98%. PCO₂ measurements were corrected to bring them to 100% equilibration efficiency conditions, by dividing the ΔPCO₂ by 0.98. This correction was small, between +2.4 ppm and -1 ppm in areas with high (480 μatm) or low (310 μatm) PCO₂, respectively. Atmospheric pressure inside the equilibrator was measured continuously with a pressure gauge, and was found to agree with ambient atmospheric pressure to within ±2 mbar.

The equilibrated air was then dried through three traps containing ice at 0°C, silica-gel, and phosphorus pentoxide, and pumped to an infrared CO₂ analyser ULTRALMAT 5E (Siemens), which measures the molar fraction of CO₂ in the atmosphere ([CO_{2 atm}]) or in equilibrated air ([CO_{2 sea}]), in parts per million (ppm). The ice and silica-gel were renewed every 4–6 h. The phosphorus pentoxide was renewed every two days. A valve was automatically switched every 10 min to air from outside, or to air from the seawater equilibrator. One [CO₂] value was recorded every minute. For each 10 min cycle, we discarded the first two measurements and the last one (which correspond to transitions), and averaged the remaining values to obtain one average [CO_{2 atm}] and one [CO_{2 sea}] value every 20 min. This was equivalent to a distance of 11 km over the ocean.

Calibrations were made once a day using two gas standards at about 200 ppm and 700 ppm, which bracket the range of [CO_{2 sea}] values encountered in the tropical Pacific. The Siemens ULTRALMAT infrared analyser has an internal software that makes the correction for non-linearity. We checked the correction by using a series of gas standards ranging from [CO₂] = 0 ppm to [CO₂] = 700 ppm delivered by a gas dilutor, and found that the error caused by non-linearity was less than 1 ppm. The drift between two consecutive calibrations was corrected assuming that it was linear with time. The instrumental error in our [CO₂] measurements (drift, instrument precision, equilibration) was ±2 ppm. The gas standards used during ECOA 1 to 5 had an accuracy of only ±2%, corresponding to ±4 ppm or ±14 ppm for the low and the high standards, respectively. We estimated the bias in these standards as the average difference between our [CO_{2 atm}] results and the results from the global atmosphere CO₂ network [Keeling, 1991 (for the American Samoa station); Conway *et al.*, 1991a–e] at the Cape Matatula, Ragged Point, Christmas Island, Key Biscayne and Terceira Island stations. The standard deviation of this difference was 3 ppm (resulting both from our system measurement error, and from the short scale variability of [CO_{2 atm}]), representing the main source of error in our data. The overall precision of our data during ECOA 1 to 5 was thus ±5 ppm.

The mole fraction of CO₂ in dry air are converted into partial pressure of CO₂ in air (pCO₂) or in air equilibrated with seawater (PCO₂), under saturated water vapour pressure at sea surface temperature, using ambient atmospheric pressure and sea surface temperature. Correction was made for the variations of CO₂ solubility with temperature using the empirical relationships of Copin-Montegut (1988, 1990). They were small in all cases, as the average temperature increase between the seawater intake and the equilibrator was less than 0.15°C. This temperature increase was continuously measured using thermistors (accuracy ±0.02°C). It was maintained at a value as small as possible, by allowing a high flow rate (50 l min⁻¹) between the seawater intake and the laboratory onboard. Only a small fraction of this flow (10 l min⁻¹) was allowed to the equilibrator.

Underway measurements of sea surface temperature (SST) and fluorescence

SST was measured continuously using a thermistor located at the seawater intake. The *in vivo* fluorescence of seawater was measured using a fluorometer (Turner model 112) fitted with a blue lamp, red-sensitive photomultiplier, blue filter 5–60 for excitation and red filter 2–64 for emission, and a high sensitivity continuous flow door. The zero of the instrument was adjusted every 4 h using freshwater as reference. Corrections were made for the drift, and the results were brought to the conditions of sensitivity corresponding to window 10X (no use was made of window 30X, which proved to be too sensitive, even in the oligotrophic waters of the south tropical Pacific).

For both SST and fluorescence, one measurement was recorded every minute. However, only one value was kept for each 20 min cycle after the processing of the CO₂ data. A failure of the fluorometer resulted in no fluorescence data during the March 1992 and June 1992 cruises.

Nitrate

Discrete seawater samples were taken every 4 h at the outflow of the fluorometer, for nitrate+nitrite concentration ([NO₃ + NO₂]) and chlorophyll determinations. The samples for [NO₃ + NO₂] were stored in 20 ml polyethylene vials previously rinsed with 0.5 N HCl, poisoned with HgCl₂, and kept frozen at –20°C. Measurements of [NO₃ + NO₂] were made at the Centre ORSTOM de Nouméa, using colorimetric methods (Strickland and Parsons, 1972). Since [NO₂] in surface seawater is usually very small, [NO₃ + NO₂] will be referred to as nitrate concentration.

Vertical profiles of temperature

Vertical profiles of temperature down to 600 m, with vertical spacing every 1.6 m, were obtained using expendable bathythermographs (XBT) launched every 4 or 6 h. These profiles were used to estimate the depth of the surface mixed layer which we arbitrarily took as the depth Z_m above which temperature was greater than SST–1°C. Gardner *et al.* (1995) defined Z_m using the depth of SST–0.1°C to study the diel variations of the mixed layer depth and their consequences, using data from a process study at a fixed station at the equator. In our large scale approach, we used a mixed layer depth definition (the depth of SST–1°C) which is commonly used in climate studies to estimate heat storage (Delcroix, 1987).

Multivariate analysis

A numerical analysis of the data was made by the Empirical Orthogonal Functions analysis (EOF), generally used to associate spatial patterns, which often represent the mark of a given phenomenon, to a time varying empirical function that describes how the intensity of this phenomenon varied over the period for which the data were analysed. We used this technique to examine how the relationships between PCO₂, SST, fluorescence, nitrate, and Z_m , vary along the shiptrack from Panama to Tahiti, and between different transects. These parameters have different dimensions and units. In order to make them homogeneous and comparable, the data were normalized (i.e. brought to average = 0,

standard deviation = 1, for data from all transects). A covariance matrix between normalized parameters was first computed, and eigenvectors were obtained after diagonalization of this matrix. We conducted the EOF analysis in such a way to obtain eigenvectors $V_{i,j}$ with co-ordinates corresponding to the parameters, and empirical orthogonal functions $F_{j,i}$ varying in space. The analysis decomposes the matrix of data in the following way:

$$P_{i,x} = \sum_{j=1}^n V_{i,j} F_{j,x} \quad (1)$$

where $P_{i,x}$ is the normalized value of parameter i at position and time x , $V_{i,j}$ is the co-ordinate of eigenvector $\#j$ for parameter i , $F_{j,x}$ is the value of the empirical orthogonal function $\#j$ at position and time x , and n is the number of observed parameters.

RESULTS

High PCO_2 was associated with low SST, high nitrate concentration and fluorescence, and shallow mixed layer during all five transects (Fig. 3), except in March 1992 when PCO_2 peaked at only $397 \mu\text{atm}$, with no sharp minima in SST nor in mixed layer depth near the equator. During August 1991 and October 1992, PCO_2 maxima were close to $480 \mu\text{atm}$ and located within 2° latitude of the equator. Lower PCO_2 was observed at the equator in November 1991 ($460 \mu\text{atm}$) and June 1992 ($437 \mu\text{atm}$). During March 1992, PCO_2 was less than $400 \mu\text{atm}$, and highest values ($397 \mu\text{atm}$) were centered at about 3°S , in the South Equatorial Current. During all transects, a striking asymmetry was observed between the northern and the southern parts: the gradient from low PCO_2 waters in the Gulf of Panama to the maximum near the equator was very abrupt ($95 \mu\text{atm}$ in 55 km in October 1992). In contrast, the PCO_2 gradient from the equator to the central south tropical Pacific was generally small and even.

Similar asymmetries between the north and the south also were observed for nitrate concentration and SST. Surface waters between 7°N and 2°N with high SST and low nitrate content were separated from the cold, nutrient-rich equatorial upwelled waters by sharp gradients. On the southern side of the equatorial upwelling, warm, nutrient-poor waters of the South Pacific subtropical gyre were found only south of 14°S . Between the equator and 14°S , progressive warming and nitrate depletion were observed.

The fluorescence of surface seawater was measured in August and November of 1991, and in October 1992. The data showed large periodic variations, which, in fact, correspond to a diel cycle, with maximum fluorescence at night and minimum during the day. This diel cycle is superimposed over a large-scale decrease of fluorescence from the equator to the south. South of 15°S , where nitrate was exhausted, fluorescence was very low. For comparison, north of 2°S , where nitrate was also exhausted, relatively high fluorescence was still recorded.

The depth of the mixed layer increased smoothly from the equator to the south. The pattern north of the equator differs in that the mixed layer thickness is less than 50 m, and showed no increase with SST, in contrast with the mixed layer south of the equator. During March 1992, the mixed layer depth was uniformly close to 75 m to the south, and 30 m to the north, with an abrupt front at the equator.

The transects made during August 1991 and October 1992 were characteristic of strong

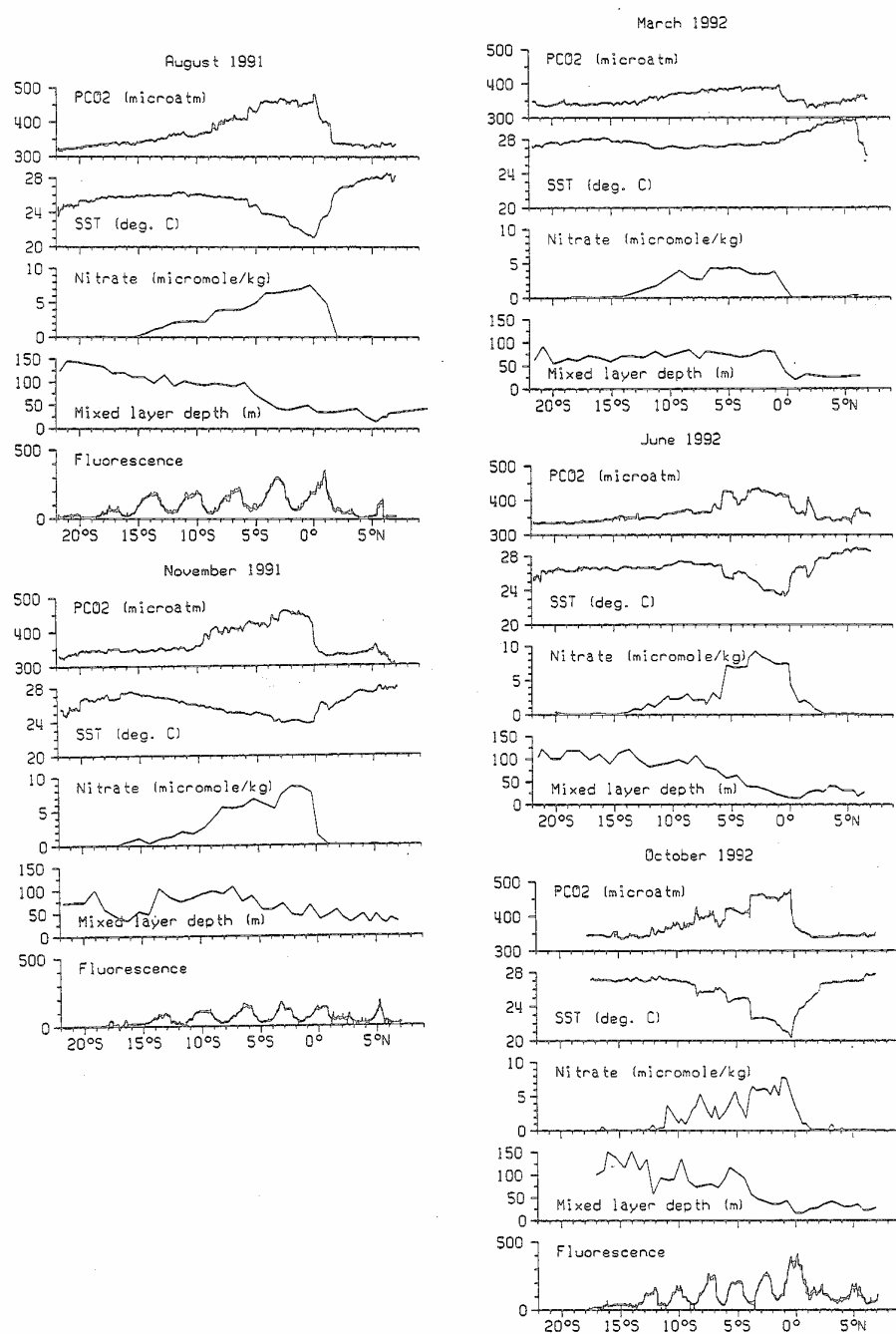


Fig. 3. Observations made during the first five ECOA transects.

equatorial upwelling, as revealed by low SST ($<21^{\circ}\text{C}$) at the equator. PCO_2 reached $480 \mu\text{atm}$, and nitrate concentration peaked at $8 \mu\text{M kg}^{-1}$. Strong signal of fluorescence was indicative of high primary production (Lorenzen, 1966). In November 1991, and June 1992, SST at the equator was about 24°C . Upwelling was weaker, and as a consequence, PCO_2 at the equator was less than in August or October. Nitrate however peaked at $9 \mu\text{M kg}^{-1}$, which was higher than in August or October. Very abnormal conditions appeared during March 1992, when El Niño conditions prevailed. Equatorial upwelling of cold, deep water had greatly reduced, as indicated by the flat curve of SST vs latitude, and by the uniform depth of the mixed layer from the equator to 21°S . However, nitrate was still present in surface water between the equator and 14°S , with maximum values of only $4 \mu\text{M kg}^{-1}$. A slight supersaturation of CO_2 (relative to the atmosphere) could still be observed in the South Equatorial Current, with a smooth maximum between $0^{\circ}40'\text{S}$ and 6°S .

Multivariate analysis

The first analysis presented here considered five descriptors (PCO_2 , fluorescence, nitrate concentration, SST and depth of the mixed layer, interpolated at the measurements of nitrate concentration), and the transects in August and November 1991, and October 1992, where these five descriptors were measured.

Of the total variance, 60.4% was accounted for by the first eigenvector (Table 1), which opposed the variations of PCO_2 , fluorescence and nitrate to SST variations. The contribution of the mixed layer depth to this eigenvector was very small. The corresponding empirical function (Fig. 4) clearly suggested the influence of the equatorial upwelling. Its shape is very similar to that of PCO_2 , and mirrors that of SST shown in Fig. 3.

The second eigenvector accounted for 20.3% of the total variance. Only the depth of the mixed layer, which had a very small weight in the first eigenvector, has a significant role here. The corresponding EOF increased to the south, as was generally the case for the depth of the mixed layer. The other descriptors, and especially PCO_2 were not sensitive to this eigenvector.

These two first eigenvectors account for 80% of the total variance, and the other ones were poorly significant. The variance of PCO_2 however was relatively strong in EOF#4, where it was positively correlated to SST, and dominated in EOF#5, where it was negatively correlated with nitrate (Table 1). Low values of F_4 and F_5 [equation (1)] make this residual variance of PCO_2 negligible.

The second analysis considered the five transects, and hence, only four descriptors,

Table 1. Multivariate analysis of the results from the transects in August 1991, November 1991 and October 1992: contributions of each parameter

	EOF#1	EOF#2	EOF#3	EOF#4	EOF#5
Percentage of total variance	60.4	20.3	12.8	4.6	1.8
PCO_2	0.54	-0.03	-0.28	0.38	0.70
Fluorescence	0.39	-0.19	0.87	0.23	-0.07
Nitrate	0.53	0.07	-0.36	0.29	-0.71
SST	-0.52	-0.04	0.00	0.85	-0.05
Depth of mixed layer	0.00	0.98	0.20	0.05	0.01

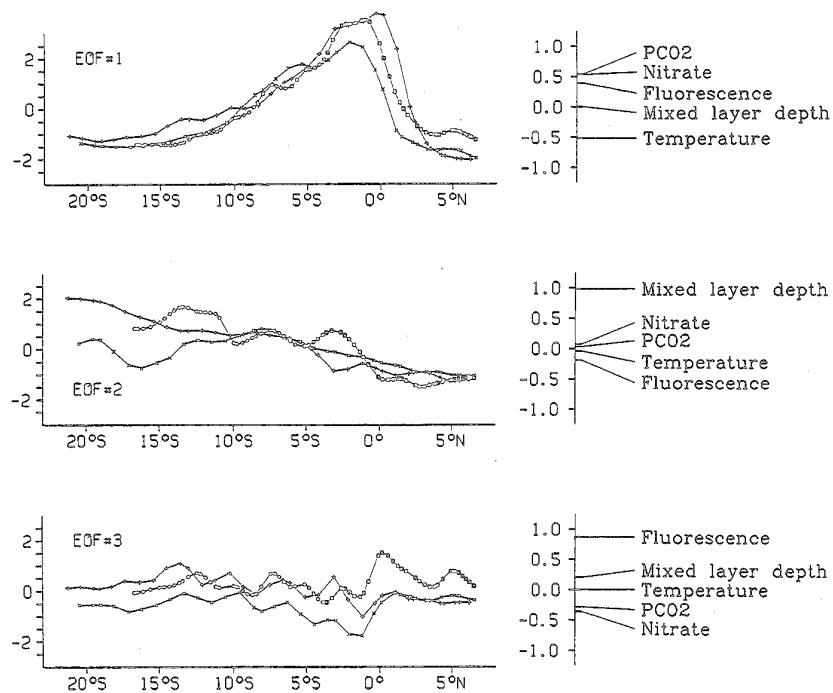


Fig. 4. Multivariate analysis of the data from three ECOA transects with fluorescence measurements. Left: empirical orthogonal functions, smoothed (+ = August 1991, \times = November 1991; squares = October 1992). Right: eigenvectors.

Table 2. Multivariate analysis of the results from the transects in August and November 1991, and March, June and October 1992: contribution of each parameter

	EOF#1	EOF#2	EOF#3	EOF#4
Percentage of total variance	64.5	24.9	8.7	1.9
PCO ₂	0.59	-0.11	0.34	-0.72
Nitrate	0.59	-0.10	0.41	0.69
SST	-0.54	-0.06	0.84	-0.04
Depth of mixed layer	0.09	0.99	0.13	-0.02

since fluorescence was not recorded in March and June 1992. The results were very similar to those from the first analysis: PCO₂ and nitrate concentration were opposed to SST in the first eigenvector (Table 2), and the depth of the mixed layer was unimportant. The corresponding EOF, which had a maximum at the equator, closely represented the

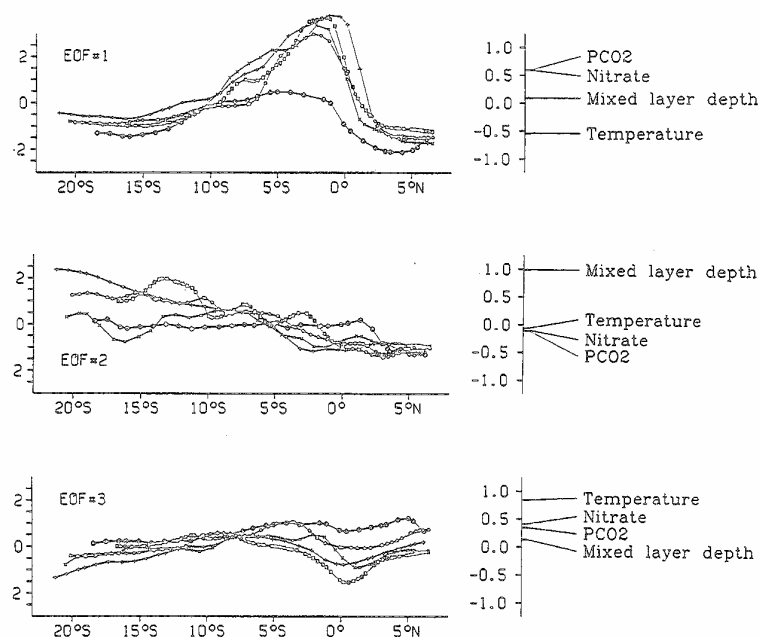


Fig. 5. Multivariate analysis of the data from the first five ECOA transects. Left: empirical orthogonal functions, smoothed (+ = August 1991; x = November 1991; open circles = March 1992; closed circles = June 1992; squares = October 1992). Right: eigenvectors.

influence of equatorial upwelling (Fig. 5). EOF#2 mostly accounted for the variations in the depth of the mixed layer. PCO₂ was the dominant descriptor in EOF#4, in which it was negatively correlated to nitrate concentration.

DISCUSSION

PCO₂ in the equatorial Pacific is very high and variable. High PCO₂ in this region is primarily caused by equatorial upwelling, which brings deep waters with high total CO₂ content to the surface. Intensity of the upwelling and the depth from which upwelled waters originate affect the variability of PCO₂. Upwelled waters are then transported by the South Equatorial Current and interact with the atmosphere. At the same time, they are heated by solar energy. PCO₂ is then modulated by the combined effects of air-sea CO₂ exchange (Murphy *et al.*, 1991; Inoue and Sugimura, 1992; Lefevre and Dandonneau, 1992; Wong *et al.*, 1993), of vertical advection of (or mixing with) deep, CO₂-rich waters, and by the thermodynamics and the biology of the water mass.

If the biological and the thermodynamical processes were affecting PCO₂ in varying proportions, the EOF analysis would separate areas or periods where the biological processes dominated from those where heating dominated. The result would be an eigenvector stretched between nitrate and PCO₂ on one side, and fluorescence on the other side, with small contribution of SST, and another eigenvector stretched between PCO₂ and SST with small contributions of fluorescence and nitrate. On the contrary, most

of PCO_2 , SST, nitrate and fluorescence variations are accounted for by the first eigenvector. This indicates that biological and thermodynamical processes generally act in a more or less constant ratio.

Highest PCO_2 values, coincident with SST minima, were found near the equator (Fig. 3) where the upwelled deep waters reach the surface. When these waters are carried by the South Equatorial Current, heating causes an increase in SST, and hence also would cause a decrease in CO_2 solubility (Weiss, 1974) and an increase in PCO_2 . What was observed in fact is a decrease of PCO_2 from the equator along the way of the ship to the southwest, i.e. in the direction of transport by the South Equatorial Current. This decrease shows that the processes that depress PCO_2 (photosynthetic carbon fixation, air-sea exchange) dominate over those that tend to increase PCO_2 (warming induced decrease of CO_2 solubility, advection of deep CO_2 -rich waters). Lefevre *et al.* (1994) indeed found that biology, inferred from nitrate consumption, plays the major role in the equatorial Pacific, while air-sea CO_2 exchange accounts for only a small part of PCO_2 variations. The southern limit of the influence of equatorial upwelling, as indicated by the presence of nitrate or high PCO_2 in surface water, is about 14°S (Fig. 3), i.e. the same as that found by Dandonneau and Eldin (1987) using chlorophyll samples collected by merchant ships along the same track.

Among the causes of PCO_2 variations, advection of deep water is the most difficult to understand using the observations collected during the ECOA transects. Nitrate concentration and PCO_2 in surface seawater are affected by mixing with (or advection of) deep waters and by biological consumption. Using the depth of the mixed layer to interpret better the variations of PCO_2 was ineffective. The mixed layer depth, arbitrarily taken as the depth where temperature equals $\text{SST}-1^\circ\text{C}$, could not be assumed in a simple way to characterize vertical advection or mixing. It also varies with horizontal divergence or convergence of the mixed layer and with internal waves, which have no effect on the chemical properties of the mixed layer water. Extreme values of the depth of the mixed layer in our data between the equator and 5°S are 75 m in March 1992, when El Niño conditions prevailed, and less than 50 m in June 1992, when equatorial upwelling started again during the Austral winter. These two transects, however, showed the lowest PCO_2 . The thermocline was shallow in June 1992, but vertical mixing with deeper water was weak, as indicated by relatively high SST at the same time (Fig. 3). Intermediate depths of the mixed layer between the equator and 5°S in August and November 1991, and in October 1992, are more favorable to high PCO_2 , because they corresponded to a weak thermocline and to subsequent intense vertical mixing with CO_2 -rich deeper waters.

North of the equator, the depth of the mixed layer was shallow on all transects (Fig. 3), as it is generally the case in the Gulf of Panama. However, unlike in the south, the strong pycnocline is a permanent barrier to vertical mixing in this area, and surface waters brought in by the North Equatorial Counter Current are generally in equilibrium with the atmosphere in PCO_2 . In contrast with temperate or high latitudes, where the mixed layer depth plays a major role in the variations of PCO_2 (Wong and Chan, 1991; Taylor *et al.*, 1991), the equatorial Pacific shows complex patterns, and knowledge of the depth of the mixed layer does not help to understand the variations of PCO_2 . We tried to conduct the analysis using $\text{SST}-0.5^\circ\text{C}$, or $\text{SST}-0.5^\circ\text{C}$, instead of $\text{SST}-1^\circ\text{C}$ (Gardner *et al.*, 1995). The contribution of the depth of the mixed layer to the variance of PCO_2 was not improved. Advection of water and its effect on PCO_2 cannot be easily described during oceanographic cruises. Lefevre *et al.* (1994) and Wanninkhof *et al.* (1995) tried to estimate the effect of horizontal advection. Complete understanding of vertical and horizontal advective

Table 3. Relationship between PCO_2 and some indicators of equatorial upwelling intensity. PCO_2 and EOF#1 are averaged between the equator and 5°S ; SST_{\min} is the minimum observed temperature, close to the equator; SOI is the Southern Oscillation Index; $\text{SLP}_{(\text{T-D})}$ is the difference in sea level pressure between Tahiti and Darwin

	$\text{PCO}_2(0^\circ\text{--}5^\circ\text{S})$ (μatm)	SST_{\min} ($^\circ\text{C}$)	EOF#1($0^\circ\text{--}5^\circ\text{S}$)	SOI	$\text{SLP}_{(\text{T-D})}$ (mb)
August 1991	456	21.4	3.56	-0.9	0.5
November 1991	438	23.8	2.94	-0.8	1.7
March 1992	380	27.3	0.09	-3.0	-0.4
June 1992	421	23.8	2.70	-1.2	-0.5
October 1992	441	21.1	3.04	-1.9	0.1
Correlation with $\text{PCO}_2(0^\circ\text{--}5^\circ\text{S})$		-0.94	0.97	0.83	0.54

tion and mixing can only be given by 3D circulation models. Vertical profiles of temperature seem here to bring no information on PCO_2 .

Fluorescence of seawater is an index of chlorophyll concentration (Lorenzen, 1965), and hence provides information on the biomass and biological activity of seawater. The fluorescence signal recorded during the ECOA transects was dominated by diel variations, with a fluorescence maximum at night, and minimum during the day, the latter resulting from inhibition at intense sunlight (Kiefer, 1973). Gardner *et al.* (1995) describe a similar diel cycle of beam transmission in the mixed layer of the equatorial Pacific, which they attribute to the downward entrainment of photosynthesized material at night. If diel variations of the fluorescence to chlorophyll ratio are known (i.e. if frequent measurements of the chlorophyll concentration are made in order to calibrate the fluorescence signal), then the fluorescence can be converted into chlorophyll concentration, and further into biomass of carbon using a (highly) variable carbon-to-chlorophyll ratio. It thus would be possible to estimate the biological storage of CO_2 . However, sedimentation of particles out of the mixed layer, together with carbon storage into zooplankton, bacteria, detritus, or dissolved organic matter, make this estimation impossible with the present data set. The fluorescence signals were empirically correlated to PCO_2 , SST and nitrate concentration, these four descriptors characterizing the equatorial upwelling (Table 1, Fig. 4).

The variations of the contribution of eigenvector #1 to the observations represents about 60% of the total variance of all parameters. The variations of this EOF with latitude, and the linear combination of mostly PCO_2 , SST, nitrate and fluorescence in this eigenvector (Figs 4 and 5), make it a synthetic representation of the influence of the equatorial upwelling. These parameters indeed have a very small weight in EOF#2, which mostly describes variations of the depth of the mixed layer. The calculated depth of the mixed layer is uncorrelated with the other parameters or with the equatorial upwelling (at least, in the way this depth was computed). Higher order EOFs can be considered as small scale noise. EOF#1 in the second multivariate analysis can thus be used to describe the variations of equatorial upwelling intensity from August 1991 to October 1992. Table 3 shows the average value of EOF#1 between the equator and 5°S for the five ECOA transects, together with the average PCO_2 in the same area, and with other commonly used indexes of upwelling intensity. SST_{\min} was taken as the minimum of observed SST; the Southern Oscillation Index (SOI) (Anonymous, 1992, 1993), and the difference of atmospheric pressure at sea-level between Tahiti and Darwin ($\text{SLP}_{(\text{T-D})}$) computed from

the monthly anomalies given in Anonymous (1992, 1993), and from the monthly mean values found in Trenberth (1984), showed weak correlation with $\text{PCO}_2(0^\circ\text{--}5^\circ\text{S})$. These two large scale synthetic indexes could not predict PCO_2 in the equatorial Pacific. In contrast, both SST_{\min} and $\text{EOF}\#1(0^\circ\text{--}5^\circ\text{S})$ were tightly correlated with $\text{PCO}_2(0^\circ\text{--}5^\circ\text{S})$ (note that $\text{PCO}_2(0^\circ\text{--}5^\circ\text{S})$ and $\text{EOF}\#1(0^\circ\text{--}5^\circ\text{S})$ are not strictly independent since PCO_2 was used to compute $\text{EOF}\#1$).

The tight correlation between SST_{\min} and $\text{PCO}_2(0^\circ\text{--}5^\circ\text{S})$ could be expected. There is a strong relationship between temperature and TCO_2 along vertical profiles, and the upwelled water at or near the equator has properties that have not yet been modified by heat storage, contact with the atmosphere or biological activity. When these upwelled waters drift away from the equator, SST and PCO_2 are modified according to processes that probably (at least in our five transects) do not change very much with time, from one transect to another. Thus, the temperature at the source of upwelled waters primarily determines PCO_2 in the area $0^\circ\text{--}5^\circ\text{S}$. Poisson *et al.* (1993) found empirical relationships between PCO_2 , SST and salinity in the Indian and Antarctic Oceans. The strong correlation found here between SST_{\min} and $\text{PCO}_2(0^\circ\text{--}5^\circ\text{S})$, if confirmed by future observations, would also permit some empirical prediction of PCO_2 in the equatorial region. However, the multivariate analyses (especially $\text{EOFs}\#4$ and $\#5$ in the first analysis, and $\#4$ in the second analysis) have shown that some minor PCO_2 variations were coupled to SST and nitrate variations (Tables 1 and 2) independently from $\text{EOF}\#1$, i.e. independently from the upwelling intensity (17% of the variance of PCO_2 is not explained by $\text{EOF}\#1$). It would be possible to assess these minor PCO_2 variations, superimposed over a mean upwelling structure, using satellite information (chlorophyll derived from satellite, SST) and knowledge of the processes which modify PCO_2 . This approach, coupled to a large scale PCO_2 distribution empirically deduced from SST at the equator, could offer a rough, simple way to predict PCO_2 in the equatorial Pacific. More measurements and a more thorough knowledge of the biological uptake of CO_2 are still necessary to achieve this goal.

CONCLUSION

The PCO_2 measurements presented here started in August 1991, under non El Niño conditions and well established equatorial upwelling. At that time, PCO_2 at the equator was close to $480\ \mu\text{atm}$. The consequence of the El Niño, which started during the 1991–1992 northern winter, was documented by the transect made in March 1992, during which PCO_2 was everywhere less than $400\ \mu\text{atm}$. Equatorial upwelling intensified in June 1992, and PCO_2 in October 1992 returned to about $480\ \mu\text{atm}$. Thus, even if the 1992 El Niño continued through 1993, as indicated by the low SOI which persisted after the end of 1991 (Anonymous, 1993), strong upwelling and high PCO_2 prevailed in October 1992; this agreed with the results from the U.S. JGOFS/EqPac cruises (Feely *et al.*, 1995).

Most of the variations of PCO_2 were coherent in parallel with nitrate concentration and fluorescence, and inversely with SST. These variations could be described after a multivariate analysis using the first eigenvector and EOF, which account for 60% of the total variance of all the observations. What was represented by this eigenvector were not elementary processes (on the contrary, heat storage would normally tend to increase PCO_2 together with SST, and chlorophyll increase would normally increase fluorescence and, oppositely, decrease PCO_2), but rather a mean pattern that resulted from the

combined action of mixing, heating, biological CO_2 uptake, and CO_2 evasion to the atmosphere. The large percentage of variance of PCO_2 explained by this mean pattern suggested that all these processes occurred simultaneously in constant proportions. In such conditions, SST alone can be used as a crude prediction of PCO_2 in the eastern equatorial Pacific. If locally, or at a given time, one particular process was stimulated, the system would evolve in a different way than the dominant one described by eigenvector#1 and EOF#1. The equatorial Pacific is a region where winds are relatively low, so that air sea exchange is not as large as suggested by ΔPCO_2 alone (Lefevre and Dandonneau, 1992). Currents are mostly zonal and steady, so that mixing probably does not vary much with time. Heat storage into the mixed layer is an even process, unlikely to exhibit large variations. On the contrary, phytoplankton growth is likely to suddenly accelerate, if the limitation by grazing (Walsh, 1976) or by lack of iron (Martin and Fitzwater, 1988) was locally removed, and if exponential growth of the phytoplankton rapidly consumed nitrate and depressed PCO_2 , as is sometimes observed in the equatorial Pacific. The most significant parameter that accounts for the influence of such outstanding events on PCO_2 would be the nitrate concentration, because the biological uptakes of carbon and nitrogen are coupled through the Redfield ratio. Actually, nitrate concentration cannot be remotely monitored, so the only way to predict PCO_2 in the equatorial Pacific is to use satellite sea-color data, which can offer a way to assess the biological CO_2 uptake.

Acknowledgements—The author is indebted to Yves Montel, Jean-Louis Crémoux, Christophe Peignon, Pascal Hamel and Eri Fukai who embarked onboard M/V *Le Rabelais* during the first five transects to watch over the equipment and make necessary sampling and calibrations, and to the officers and crew whose services were often called on. The Directors of the Compagnie Générale Maritime kindly smoothed all the difficulties during this monitoring experiment. The software for data recording and automatic control of the valves was developed by Jacques Grelet, from the Centre ORSTOM de Nouméa. The author also thanks the reviewers for useful comments. The launching of XBTs is supervised by the SURTROPAC Group in Nouméa, who processed the data and made them available. Nutrients and chlorophyll measurements are made by the FLUPAC group at the Centre ORSTOM de Nouméa. This program is part of the French PNEDC/ CO_2 program, and is supported by ORSTOM and by European contract Escoba.

REFERENCES

- Anonymous (1992) Climate Diagnostics Bulletin, July 1992. U.S. Department of Commerce, National Oceanic and Atmospheric Administration, National Weather Service, National Meteorological Center, Washington, report no. 92/7, 68 pp.
- Anonymous (1993) Climate Diagnostics Bulletin, July 1993. U.S. Department of Commerce, National Oceanic and Atmospheric Administration, National Weather Service, National Meteorological Center, Washington, report no. 93/7, 81 pp.
- Bacastow R. B., J. A. Adams, C. D. Keeling, D. J. Moss, T. P. Whorf and C. S. Wong (1980) Atmospheric carbon dioxide, the Southern Oscillation, and the weak 1975 El Niño. *Science*, 210, 66–68.
- Broecker W. S., J. R. Ledwell, T. Takahashi, R. Weiss, L. Merlivat, L. Memery, T. H. Peng, B. Jahne and K. O. Munnich (1986) Isotopic versus micrometeorologic ocean CO_2 fluxes: a serious conflict. *Journal of Geophysical Research*, 91, 10,517–10,527.
- Conway T. J., P. P. Tans and L. S. Waterman (1991a) Atmospheric CO_2 —modern record, Christmas Island. Carbon Dioxide Information Analysis Center, Oak Ridge National Laboratory, Oak Ridge, Tennessee, U.S.A., pp. 76–79.
- Conway T. J., P. P. Tans and L. S. Waterman (1991b) Atmospheric CO_2 —modern record, Key Biscayne. Carbon Dioxide Information Analysis Center, Oak Ridge National Laboratory, Oak Ridge, Tennessee, U.S.A., pp. 88–91.
- Conway T. J., P. P. Tans and L. S. Waterman (1991c) Atmospheric CO_2 —modern record, Ragged Point.

- Carbon Dioxide Information Analysis Center, Oak Ridge National Laboratory, Oak Ridge, Tennessee, U.S.A., pp. 124–127.
- Conway T. J., P. P. Tans and L. S. Waterman (1991d) Atmospheric CO₂—modern record, Terceira Island. Carbon Dioxide Information Analysis Center, Oak Ridge National Laboratory, Oak Ridge, Tennessee, U.S.A., pp. 140–143.
- Conway T. J., P. P. Tans and L. S. Waterman (1991e) Atmospheric CO₂—modern record, Cape Matatula. Carbon Dioxide Information Analysis Center, Oak Ridge National Laboratory, Oak Ridge, Tennessee, U.S.A., pp. 68–71.
- Copin-Montegut C. (1985) A method for the continuous determination of the partial pressure of carbon dioxide in the upper ocean. *Marine Chemistry*, 17, 13–21.
- Copin-Montegut C. (1988) A new formula for the effect of temperature on the partial pressure of CO₂ in seawater. *Marine Chemistry*, 25, 29–37.
- Copin-Montegut C. (1990) Corrigendum. *Marine Chemistry*, 27, 143–144.
- Dandonneau Y. and G. Eldin (1987) Southwestward extent of chlorophyll-enriched waters from the Peruvian and equatorial upwellings between Tahiti and Panama. *Marine Ecology Progress Series*, 38, 283–294.
- Delcroix T. (1985) Net heat gain of the tropical Pacific Ocean computed from subsurface ocean data and wind stress data. *Deep-Sea Research*, 34, 33–43.
- Eldin G. and A. Morliere (1992) Acoustic Doppler current profiling along the Pacific equator from 95°W to 165°E. *Geophysical Research Letters*, 19, 913–916.
- Feely R. A., R. H. Gammon, B. A. Taft, P. E. Pullen, L. S. Waterman, T. J. Conway, J. F. Gendron and D. P. Wisegardner (1987) Distribution of chemical tracers in the eastern equatorial Pacific during and after the 1992–1993 El Niño/Southern Oscillation Event. *Journal of Geophysical Research*, 92, 6545–6558.
- Feely R. A., R. Wanninkhof, C. E. Cosca, P. P. Murphy, M. F. Lamb and M. D. Steckley (1995) CO₂ distributions in the equatorial Pacific during the 1991–1992 ENSO Event. *Deep-Sea Research II*, 42, 365–386.
- Gardner W. D., S. P. Chung, M. J. Richardson and I. D. Walsh (1993) The oceanic mixed layer pump in the equatorial Pacific. *Deep-Sea Research II*, 42, 757–775.
- Gaudry A., P. Monfray, G. Polian, G. Bonsang, B. Ardouin, A. Jegou and G. Lambert (1991) Non-seasonal variations of atmospheric CO₂ concentrations at Amsterdam Island. *Tellus*, 43B, 136–143.
- Inoue H. Y. and Y. Sugimura (1992) Variations and distributions of CO₂ in and over the equatorial Pacific during the period from the 1986/88 El Niño event to the 1988/89 La Niña event. *Tellus*, 44B, 1–22.
- Keeling C. D. (1968) Carbon dioxide in surface ocean waters. 4. Global distribution. *Journal of Geophysical Research*, 73, 4543–4553.
- Keeling C. D. (1991) Atmospheric CO₂—modern record, American Samoa. Carbon Dioxide Information Analysis Center, Oak Ridge National Laboratory, Oak Ridge, Tennessee, U.S.A., pp. 16–19.
- Keeling C. D. and R. Revelle (1985) Effects of El Niño/Southern Oscillation on the atmospheric content of carbon dioxide. *Meteoritics*, 20, 437–450.
- Keeling C. D., N. W. Rakestraw and L. S. Waterman (1965) Carbon dioxide in surface waters of the Pacific Ocean. 1. Measurements of the distribution. *Journal of Geophysical Research*, 70, 6087–6097.
- Kiefer D. A. (1973) Fluorescence properties of natural phytoplankton populations. *Marine Biology*, 22, 263–269.
- Lefevre N. and Y. Dandonneau (1992) Air–sea CO₂ fluxes in the equatorial Pacific in January–March 1991. *Geophysical Research Letters*, 19, 2223–2226.
- Lefevre N., C. Andrie, Y. Dandonneau, G. Reverdin and M. Rodier (1994) PCO₂, chemical properties and estimated new production in the equatorial Pacific in January–March 1991. *Journal of Geophysical Research*, 99, 12,639–12,654.
- Lorenzen C. L. (1966) A method for the continuous measurement of *in vivo* chlorophyll concentration. *Deep-Sea Research*, 13, 223–227.
- Martin J. H. and S. E. Fitzwater (1988) Iron deficiency limits phytoplankton growth in the northeast Pacific subarctic. *Nature*, 331, 341–343.
- Murphy P. P., R. A. Feely, R. H. Gammon, D. E. Harrison, K. C. Kelly and L. S. Waterman (1991) Assessment of the air–sea exchange of CO₂ in the South Pacific during austral autumn. *Journal of Geophysical Research*, 96, 20,455–20,465.
- Murray J. W., M. W. Leinen, R. A. Feely, J. R. Toggweiler and R. Wanninkhof (1992) EQPAC: a process study in the Central Equatorial Pacific. *Oceanography*, 5, 134–142.
- Philander G. (1989) *El Niño, La Niña, and the Southern Oscillation*. Academic Press, San Diego, CA, U.S.A., 293 pp.

- Strickland J. D. H. and T. Parsons (1972) A practical handbook of seawater analysis. *Fisheries Research Board of Canada Bulletin*, 167, 1–310.
- Taylor A. H., A. J. Watson, M. S. Ainsworth, J. E. Robertson and D. R. Turner (1991) A modelling investigation of the role of phytoplankton in the balance of carbon at the surface of the North Atlantic. *Global Biogeochemical Cycles*, 5, 151–171.
- Trenberth K. E. (1984) Signal versus noise in the Southern Oscillation. *Monthly Weather Review*, 112, 326–332.
- Walsh J. J. (1976) Herbivory as a factor in patterns of nutrient utilization in the sea. *Limnology and Oceanography*, 21, 1–13.
- Wanninkhof R., R. A. Feely, D. K. Atwood, G. Berberian, D. Wilson, P. P. Murphy and M. F. Lamb (1995) Seasonal and lateral variations in carbon chemistry of surface water in the eastern equatorial Pacific during 1992. *Deep-Sea Research*, 42, 387–409.
- Weiss R. F. (1974) Carbon dioxide in water and seawater: the solubility of a non-ideal gas. *Marine Chemistry*, 2, 203–215.
- Wong C. S. and H. Y. Chan (1991) Temporal variations in the partial pressure and flux of CO₂ at Ocean Station P in the subarctic northeast Pacific Ocean. *Tellus*, 43B, 206–223.
- Wong C. S., Y. H. Chan, J. S. Page, R. D. Bellegay and K. G. Pettit (1984) Trends of atmospheric CO₂ over Canadian WMO background stations at ocean weather station P, Sable Island, and Alert. *Journal of Geophysical Research*, 89, 9527–9539.
- Wong C. S., Y. H. Chan, J. S. Page, G. E. Smith and R. D. Bellegay (1993) Changes in equatorial CO₂ flux and new production estimated from CO₂ and nutrient levels in Pacific surface waters during the 1986/87 El Niño. *Tellus*, 45B, 64–79.
- Wyrtki K. (1981) An estimate of equatorial upwelling in the Pacific. *Journal of Physical Oceanography*, 11, 1205–1214.